J. Eur. Opt. Society-Rapid Publ. 2025, **21**, 51
© The Author(s), published by EDP Sciences, 2025
https://doi.org/10.1051/jeos/2025046
Available online at: https://jeos.edpsciences.org

Journal of the European Optical Society-Rapid Publications

RESEARCH ARTICLE OPEN ACCESS

Watt-level polarization-maintaining Er^{3+}: ZBLAN fiber laser tunable from 3.4 µm to 3.7 µm

Saad Hatim[1], Kirill Eremeev[1], Tristan Guezennec[1], Marie Guionie[1], Saïd Idlahcen[1], Pierre-Henry Hanzard[1], Thomas Godin[1], Thibaut Sylvestre[2], Pavel Loiko[3], Patrice Camy[3], Thibaud Berthelot[4], Solenn Cozic[4], Samuel Poulain[4], and Ammar Hideur[1,*]

[1] CORIA UMR6614, CNRS-INSA-Université de Rouen, Normandie Université, 76801 Saint Etienne du Rouvray, France
[2] Institut FEMTO-ST, CNRS-Université de Franche-Comté, 25030 Besançon, France
[3] CIMAP UMR6252 CEA-CNRS-ENSICAEN, Université de Caen Normandie, 14050 Caen, France
[4] Le Verre Fluoré, rue Gabriel Voisin, Campus de Ker-Lann, 35170 Bruz, France

Received 5 October 2025 / Accepted 12 November 2025

Abstract. We demonstrate a linearly polarized Er^{3+}: ZBLAN fiber laser in the dual wavelength pumping scheme for laser emission in the 3400–3700 nm spectral band. The laser is based on a polarization-maintaining heavily erbium-doped ZBLAN fiber dually pumped at 976 nm and 1975 nm. Continuously tunable lasing is obtained from 3380 nm to 3717 nm by using a diffraction grating in combination with a high reflectivity output coupler. Using a low reflectivity output coupler, watt-level output powers are achieved for the first time from a PM-fiber laser in the 3400–3600 nm wavelength range. The polarization extinction ratio (PER) of the output beam is greater than 21 dB over the whole tuning range.

Keywords: Polarization-maintaining, Fiber laser, Erbium, ZBLAN, Mid-infrared, Dual wavelength pumping.

1 Introduction

Broadly tunable lasers operating in the mid-infrared (MIR) spectral region, particularly between 3000 and 4000 nm, have attracted significant attention due to their wide range of applications. These include remote sensing of greenhouse gases such as methane [1] and polymer materials processing owing to the strong absorption by C–H bonds in this region, medical diagnostics via breath analysis, laser surgery, and molecular fingerprinting in spectroscopy [2–6]. While various platforms – such as optical parametric oscillators/amplifiers, quantum cascade lasers, and supercontinuum sources – can access this spectral region [7–9], their complexity, high cost, and limited power scalability restrict their practical implementation. Rare-earth-doped fluoride fiber lasers, such as zirconium fluoride (ZrF_4), offer a compelling alternative, combining excellent beam quality with high power scalability. Among rare-earth dopants, Erbium (Er^{3+}) ions are especially attractive due to their broad emission centered around 3500 nm from the $^4F_{9/2} \rightarrow {}^4I_{9/2}$ transition as shown in Figure 1a. Direct pumping of this transition at 650 nm yielded low efficiencies due to a low Stokes efficiency of only 18% [11]. However, the approach of dual-wavelength pumping (DWP), introduced by Henderson-Sapir *et al.* [12], has significantly enhanced the development MIR Er^{3+} fiber lasers, enabling multi-watt continuous-wave (CW) operation with high efficiency [13, 14]. In this scheme, ground-state absorption at 976 nm populates the $^4I_{11/2}$ level, which is further excited by a second pump at 1975 nm to reach the $^4F_{9/2}$ upper laser level, enabling laser emission from 3500 to 3800 nm. Following this progress, considerable research has focused on scaling CW output power and pushing the laser wavelength to the edge of the gain spectrum. First tunable laser operation on the $^4F_{9/2} \rightarrow {}^4I_{9/2}$ transition across the 3330–3780 nm wavelength range was demonstrated by Henderson-Sapir *et al.* using diffraction gratings [15]. Further extension of the laser emission to long wavelengths beyond 3800 nm was achieved by Zhang *et al.*, reaching 3810 nm with 45 mW output power [16]. On the other hand, single-frequency operation in the 3370–3720 nm range was achieved using a germanium-based etalon [17]. Besides the diffraction gratings, wavelength selection can also be achieved using high-transmission bandpass filters (BPF) or fiber Bragg gratings (FBG) [10, 18]. For instance, Zhang *et al.* demonstrated a 4.5 W CW laser at 3780 nm with 6.5% overall efficiency using a low-Er^{3+}-doped fiber and a high transmission BPF [18], which was superior to the 2 W reported previously using FBG [10]. Low-Erbium doped fibers minimize the thermal load, enabling integration into

* Corresponding author: hideur@coria.fr

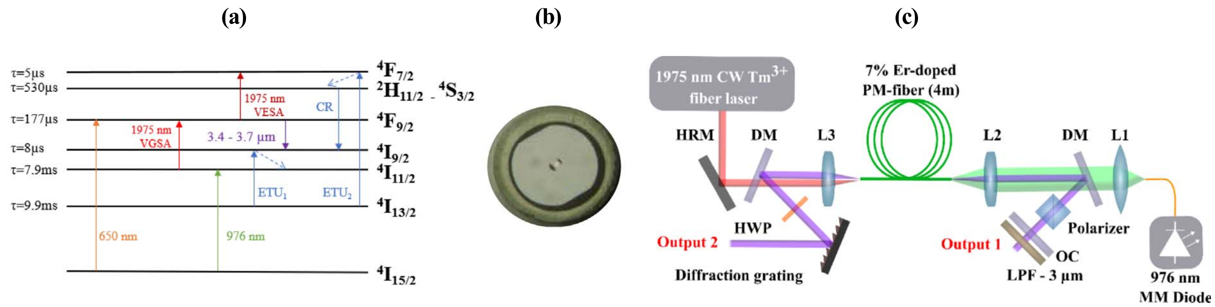

Figure 1. (a) Er^{3+} ion energy levels in ZBLAN, energy transfers and lifetimes (values extracted from [10]). VGSA: Virtual Ground State Absorption; VESA: Virtual Excited State Absorption; CR: Cross Relaxation; ETU: Energy Transfer Upconversion. (b) Microscopic image showcasing the double clad design and the presence of two air holes. (c) Experimental scheme of the bidirectional DWP laser. DM: Dichroic mirror. HRM: Highly reflective mirror. L1: Achromatic lens. L2, L3: ZnSe lenses. LPF: Long pass filter. HWP: Half wave plate. OC: Output coupler.

monolithic architectures with FBG and eliminating the need for active cooling [19]. Conversely, Maes *et al.* [20] demonstrated a 28% efficiency and 3.4 W output at 3420 nm using heavily Er^{3+}-doped fibers, surpassing the overall optical efficiency achieved with lower dopant levels. Consistent with Ref. [20], under insufficient 976 nm pumping, low-Erbium-doped fibers undergo rapid quenching driven by Excited State Absorption (ESA) from $^4F_{9/2}$ to $^4F_{7/2}$. By contrast, heavily doped fibers exhibit higher lasing thresholds but maintain larger slope efficiencies. The mitigated quenching at high Er^{3+} concentration is attributed to strengthened energy-transfer pathways from the $^2H_{11/2}$ and $^4S_{3/2}$ manifolds, which suppress ESA into $^4F_{7/2}$ and enhance the quantum efficiency of the 3500 nm transition. Despite tremendous advances in terms of output power and slope efficiency, 3500 nm lasers based on standard double-clad fibers suffer from strong environmental instability due to their sensitivity to mechanical vibrations and temperature variations that induce changes in the fiber birefringence. The use of Polarization Maintaining (PM)-fibers is the most efficient approach to build environmentally-stable laser systems with linearly polarized output beams which are very suitable for several applications such as material processing and spectroscopy [21, 22]. While tunable operation in PM fibers has been demonstrated at 2800 nm [23, 24], and linear polarized CW lasing at 3,460 nm has been achieved with PM Er^{3+}: ZrF_4 fibers [25], high-power laser operation beyond 3500 nm has not yet been reported. In this work, we explore for the first-time laser emission beyond 3500 nm from a polarization maintaining heavily erbium-doped fiber laser. We thereby demonstrate a linearly polarized watt-level fiber laser widely tunable from 3400 nm to 3700 nm. The DWP-based laser delivers a maximum power of 1.61 W at 3500 nm in a single-mode beam with a PER of 21 dB.

2 Material and methods

The experimental setup of our DWP Er^{3+}-doped fiber laser is shown in Figure 1c. The gain medium, a 4 m long double-clad (double D-shaped) 7 mol% Er^{3+}: ZrF_4 PM fiber (Le Verre Fluoré, 15/240 × 260 μm), is used in a bidirectional dual-wavelength pumping scheme. It has a core/clad numerical aperture (NA) of 0.125 allowing single mode operation over the whole spectral band 3300–3800 nm (cut-off wavelength at 2600 nm). The birefringence of the fiber is ensured by two air gaps around the core (L_B = 38 mm at 2880 nm), see Figure 1b. Both facets of the fiber have AlF3 based end-caps with a length of 600 μm and were cleaved at an angle of 14° to avoid parasitic lasing due to Fresnel reflections. The 976 nm pump is a 30 W laser diode (976LD-4-0-0, Aerodiode, France) pigtailed with a multimode fiber featuring a core diameter of 105 μm and a NA of 0.22, collimated using an achromatic lens (L1, $f = 10$ mm).

The 1975 nm pump is a commercial Tm^{3+} single-mode (NA = 0.15) fiber laser (IFL30, Futonics GmbH, Germany) delivering up to 30 W and is guided using a highly reflective mirror (Layertec, $R > 95\%$ at 1975 nm). The 976 nm pump is coupled into the fiber's cladding using a ZnSe lens (L2, $f = 25$ mm) while the 1975 nm pump is launched into the core of the fiber using a second ZnSe lens (L3, f = 12 mm) to ensure high pump absorption. The laser cavity is built using two dichroic mirrors placed at 22° (Optoman, 95% transmission for 976 nm and 1975 nm, more than 99% reflectivity for 3300–4000 nm). The first arm of the cavity contains a diffraction grating (Thorlabs GR1325-30035, grating diffraction efficiency of 85% at 3500 nm with less than 2% variations in the 3300–3750 nm range) mounted in Littrow configuration and allowing wavelength selection by reinjecting the first order of diffraction into the fiber. A half waveplate (Thorlabs WPLH05M-3500) is used to tailor the polarization orientation angle of the laser beam in order to minimize the losses through the grating' zero-order diffraction (Output 2). The second arm of the cavity contains a linear polarizer in which its polarization axis is carefully aligned to the slow polarization axis of the PM fiber to ensure polarization state preservation. The cavity is closed by an output coupler (Optoman, T_{OC} = 30%, T_{OC} = 50% and T_{OC} = 70%, transmission for 3300–4000 nm). The output of the laser is then collected after a 3000 nm long-pass filter (Spectrogon – LP-3000 nm) to ensure that no residual pump or laser emission at 2800 nm is considered during measurements (Output 1). It is worth noting that the 2800 nm colasing emission, arising from

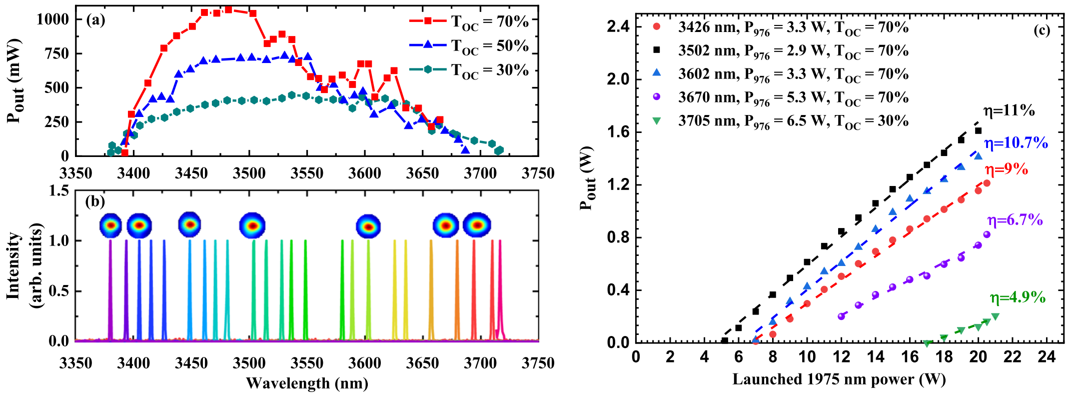

Figure 2. (a) Laser wavelength tunability for the three output couplers and corresponding output power for fixed powers of 7.4 W and 20 W for the 976 nm and 1975 nm pumps, respectively. (b) Normalized laser emission spectra over the tuning range. Insets: Beam profile of the laser output at selected wavelengths in the case of T_{OC} = 30%. (c) Output power curves and optical efficiencies versus launched 1975 nm pump power for different laser emission wavelengths at fixed 976 pump power P_{976}.

parasitic reflections on the fiber facets, only appears near laser threshold and it is totally inhibited for 1975 nm pumping levels higher than 1.2 times the pumping threshold. The laser spectra were acquired using a Fourier transform optical spectrum analyzer (Thorlabs OSA 205C) with a spectral resolution of 0.5 nm at 3500 nm. The laser power was measured using a sensitive thermal power-meter (Thorlabs S405C, 100 μW – 5 W power range).

3 Results and discussion

3.1 Cavity alignment and fiber length optimization

The alignment starts by optimizing the 1975 nm pump coupling into the fiber core in an open-cavity configuration (without feedback mirrors). The fiber length was then selected to yield more than 90% absorption at 1975 nm under approximately 5W of 976 nm pump power. Next, the cavity was closed with reflective mirrors, and alignment was refined by maximizing the 3500 nm emission. After optimization, a slight decrease in 1975 nm pump absorption was observed, due to decreasing of injection efficiency from 90% to 78%. An initial length of 2.5 m was implemented based on Ref. [20] predictions for optimal fiber length/doping for 3500 nm emission in a 7 mol% standard Er^{3+}-doped fiber, but attempts to achieve lasing with our PM fiber were unsuccessful. Increasing the fiber length to 4 m enabled stable 3500 nm lasing with residual 1975 nm pump of below 10%. The longer optimum is likely due to higher linear losses in the PM fiber, which reduce the effective gain relative to the standard-fiber case.

3.2 Laser tuning

Our initial study focused on the wavelength tunability of the ZBLAN fiber laser obtained by adjusting the diffraction grating, for different output couplers. Figure 2a summarizes the tuning range for the three output couplers used in this study and the corresponding output power. Pump powers were fixed at 7.4 W and 20 W for the 976 nm pump and 1975 nm pump, respectively in order to observe the laser tuning in each case. As expected for the $^4F_{9/2} \rightarrow {}^4I_{9/2}$ four level transition of Er^{3+} ions in ZBLAN, a broad tuning range of 337 nm (260 nm at FWHM) around 3550 nm is obtained in the case of T_{OC} = 30%. However, the tuning bandwidth is narrower than that obtained with non-PM fibers [15, 16]. It is worth noting that although the $^4F_{9/2} \rightarrow {}^4I_{9/2}$ transition exhibits a broadband emission around 3550 nm, its low emission cross section calls for low cavity losses and high fiber's optical transmission to achieve high efficiency from this transition. Experimental measurements show that our Erbium-doped PM fiber exhibits higher losses (~43 dB/km [24]) than the standard double-clad version (~30 dB/km [26]) thus making it difficult to achieve lasing below 3380 nm and beyond 3720 nm. Moreover, the lower efficiency of the diffraction grating combined with the increasing ZBLAN losses for wavelengths beyond 3700 nm (compared to 3500 nm) poses further limitations to achieve stable lasing at longer wavelengths. Figure 2b highlights the normalized emission spectra of the laser showing excellent continuous tuning between 3380 nm and 3717 nm, in the case of T_{OC} = 30%. Using lower-cavity losses (lower output coupling) provides broader tuning range but at the cost of lower efficiency. The output coupling value of 30% is found to be a good compromise enabling high efficiency on a broad wavelength range. Implementing an output coupler with T_{OC} = 70% enabled the emission of linearly-polarized laser light with watt-level output powers in the 3400–3600 nm wavelength range, more than five times higher than the performance previously demonstrated at 3500 nm [25]. While tuning the laser, a beam profiler (Pyrocam IIIHR) was used to observe the output beam spot shape in the far field as showcased in Figure 3b inset. Along with laser stability, a good quality single mode beam corresponding to a gaussian distribution is observed on the output for all wavelengths of interest. To confirm the power stability and beam characteristics, we monitored the output power, and performed M^2 measurements at a fixed wavelength of 3500 nm for an output coupling ratio of 70%. The average output power of about 1W is measured over almost 5 h, see Figure 3a.

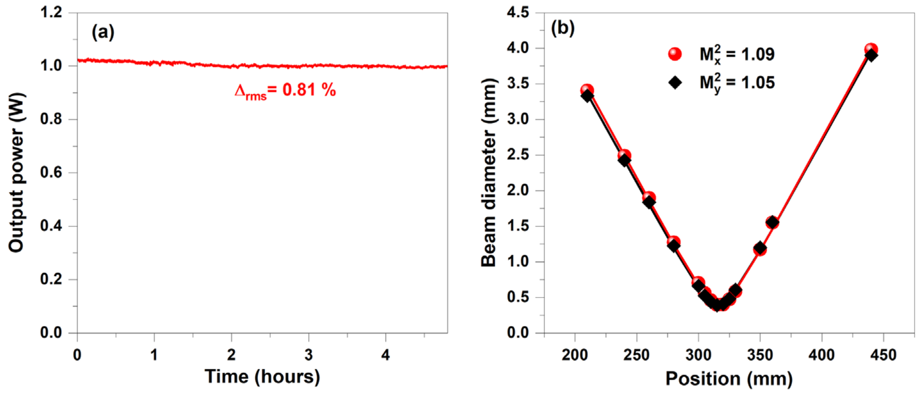

Figure 3. Laser performances at 3500 nm for 70% output coupling ratio: (a) Laser power stability over 5 h for 1 W output power. (b) M^2 measurements of the output laser beam.

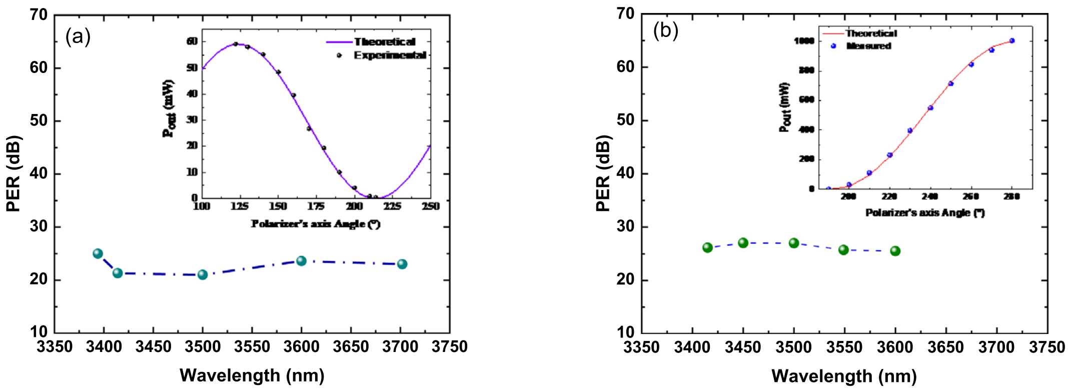

Figure 4. PER measurements as a function of wavelength in the case of $T_{OC} = 30\%$ (a) and $T_{OC} = 70\%$ (b). Insets: Typical linear polarization measurement results with theoretical fit (Malus' law) for laser emission at 3414 nm with $T_{OC} = 30\%$ (a) and for laser emission at 3500 nm with $T_{OC} = 70\%$ (b).

After a slight initial decrease due to thermal stabilization, the power remained stable throughout the experiment with an overall rms deviation of 0.81%. The M^2 measurement was performed using a 200 mm focal length CaF_2 lens and our Pyrocam. Figure 3b shows the results which highlight the excellent beam quality, with an M^2 of 1.09 (resp. 1.05) on the x-axis (resp. y-axis). This slight astigmatism is most likely due to the PM operation of the fiber. The air holes surrounding the core deconfine the mode on one axis, resulting in a slightly elliptical mode.

3.3 Output power scaling

Figure 2c shows the evolutions of the output powers at key wavelength points with respect to the launched pump power at 1975 nm for fixed 976 nm pump power. Increasing the 976 nm pump power allows to supply sufficient population on the $^4I_{11/2}$ and thus more gain for lasing at long wavelengths. The pumping power at this wavelength is relatively low compared to the pumping needed for low doped Erbium fluoride fibers as they exhibit rapid quenching effects when increasing the 1975 nm pump power [19, 20]. At the central wavelength of 3500 nm, a maximum output power of 1.61 W of polarized laser light was achieved for a pump power of 20 W at 1975 nm, which corresponds to an efficiency of 11% (with respect to the 1975 nm pump power). We note that the calculated slope efficiency with respect to the 1975 nm pump power injected into the fiber is about 14%. This watt-level power was achieved for the whole range of 3400–3600 nm although with varying efficiencies. Beyond this wavelength range, high output powers were also achieved, for instance at 3670 nm with 830 mW, which corresponds to an efficiency of 6.7%. Note that even if heavily doped Erbium fluoride fibers do not exhibit rapid quenching effects, the heavy doping induces rapid heating compared to low doped fibers. This effect combined with the high thermal expansion coefficient of fluoride glass (200×10^{-7} K^{-1}) puts the fiber facets at risk of damage limiting further power scaling. This also induces a mechanical "shift" of the fiber core making it necessary to adjust the injection of the 1975 nm pump when increasing the pump power. This explains the small fluctuations that can be seen on the experimental measurements when increasing the 1975 nm pump power. For pump powers higher than 21 W, strong output power fluctuations are observed which is usually an indication that the fiber facet is starting to get damaged. To avoid any fiber damage, we explored the pump power range below 21 W where the laser exhibited an excellent output power stability over the whole wavelength range.

3.4 Polarization extinction ratio (PER)

The output beam PER monitoring was done using a second polarizer mounted on a rotation stage. Figure 4a shows PER measurements at points of interest of the tunable fiber laser in the case of $T_{OC} = 30\%$. A typical measurement of the power transmission through the polarizer versus its orientation angle for laser emission at 3414 nm is presented as well (inset). The experimental curve is well fitted with a Malus law indicating that laser emission is linearly polarized with a PER of 21 dB. The measured PER was not the same for the entire tuning range and this could be attributed to the fact that the polarization components as well as the PM-fiber did not exhibit the same polarization behavior for all wavelengths. While the polarization components exhibit different efficiencies for each wavelength, the PM fiber is more sensitive to heat loads on the fiber tips. This heating contributes to thermal expansion of the fiber facet mentioned before that could induce a shifting of not only the core, but of the slow and fast polarization axis. Ruffin *et al.* observed such an effect while working with highly birefringent silica fibers under different temperature conditions [27]. It is then possible that the higher thermal expansion of fluoride fibers exhibits the same behavior just at lower temperatures due to rapid expansion. Thus, inducing different measurement results as reaching stability for each wavelength requires different pump powers and by consequence different expansions of the fiber facet. Consequently, the lowest measured PER is 21 dB at 3500 nm and the highest is 25 dB measured at 3394 nm, thus giving an average of approximately 22.8 dB over the tuning range. Measurements performed at high output coupling ($T_{OC} = 70\%$) yield excellent results, with PER values exceeding 25.5 dB across the 3.4–3.6 μm wavelength range, see Figure 4b. This improvement in PER can be attributed to a reduced intracavity thermal load resulting from a higher power extraction from the cavity compared to the low output coupling case.

4 Conclusion and prospects

In summary, we have demonstrated a widely tunable linearly-polarized fiber laser based on a highly-birefringent heavily Erbium-doped fluoride fiber. The maximum tuning range achieved in a low losses' cavity was 337 nm around 3550 nm. By increasing the output coupling, watt-levels of continuous wave powers were achieved in the 3400–3600 nm wavelength range with linearly polarized laser emission. A polarization extinction ratio of more than 25 dB is achieved over the whole tuning range. The laser delivers a high-quality single mode beam and is stable for hours in a laboratory environment. Given the growing interest of these fibered devices in the MIR, integrating the proposed setup into a monolithic structure by the use of femtosecond written fiber Bragg gratings, pump combiners and ZBLAN fibre-based components could serve to make the setup more compact and facilitate handling by users, these design choices are currently under investigation for future improvements. Moreover, the development of lightly-erbium doped PM fibers will open the path for power scaling by limiting the thermal effects. Nevertheless, this wide tunability combined with watt-level powers of polarized laser emission in the mid-infrared is a first demonstration of the capability of these sources to be implemented in various applications such as dual-comb spectroscopy.

Funding

This work has received support from the French Agency for Research (ANR) under projects MIR-SESAM (ANR-23-CE24-0014) and Labex EMC3 (ANR-10-LABX-09), the Normandy region and the European Regional Development Fund.

Conflicts of interest

The authors declare no conflicts of interest.

Data availability statement

Data underlying the results presented in this paper are not publicly available at this time but may be obtained from the authors upon reasonable request.

Author contribution statement

Conceptualization, S.H., Tr.G., K.E., M.G., S.I., and A.H.; Methodology, S.H. and A.H.; Validation, S.I., P.H.H, Th.G. and A.H.; Formal Analysis, S.H., Tr.G., K.E. and A.H.; Investigation, S.H., Tr.G., K.E. and A.H.; Resources, S.C., T.B., S.P., T.S., P.L., P.C., P.H.H, Th.G. and A.H.; Data Curation, S.H.; Writing – Original Draft Preparation, S.H.; Writing – Review & Editing, S.H., K.E., Tr.G., M.G., S.I., P.H.H, Th.G. and A.H.; Supervision, S.I., P.H.H, Th.G. and A.H.; Project Administration, S.I., P.H.H, Th.G. and A.H.; Funding Acquisition, P.H.H, Th.G. and A.H.

References

1 Pleau L, Fortin V, Maes F, Vallée R, Bernier M, Tunable all-fiber laser for remote sensing of methane near 3.4 μm, in Conference on Lasers and Electro-Optics Europe and European Quantum Electronics Conference, OSA Technical Digest (Optica Publishing Group, 2019), paper cj_5_2.

2 Selvaraj R, Vasa NJ, Nagendra SMS, Mizaikoff B, Advances in mid-infrared spectroscopy-based sensing techniques for exhaled breath diagnostics, Molecules 25, 2227 (2020). https://doi.org/10.3390/molecules25092227.

3 Larson E, Hines M, Tanas M, Miller B, Coleman M, Toor F, Mid-infrared absorption by soft tissue sarcoma and cell ablation utilizing a mid-infrared interband cascade laser, J. Biomed. Opt. 26(4) 043012 (2021). https://doi.org/10.1117/1.JBO.26.4.043012.

4 Pangerl J, Sukul P, Rück T, Escher L, Miekisch W, Bierl R, Matysik F-M, Photoacoustic trace-analysis of breath isoprene and acetone via interband- and quantum cascade lasers, Sens. Actuators B: Chem. 424, 136886 (2025). https://doi.org/10.1016/j.snb.2024.136886.

5 Bérubé JP, Frayssinous C, Lapointe J, Duval S, Fortin V, Vallée R, Direct inscription of on-surface waveguides in polymers using a mid-IR fiber laser, Opt. Express 27(21), 31013–31022 (2019). https://doi.org/10.1364/OE.27.031013.

6 Vodopyanov KL, in Laser-based mid-infrared sources and applications (John Wiley & Sons, 2020). https://doi.org/10.1002/9781119074557.ch7.

7 Jiao Y, Jia Z, Zhang C, Guo X, Meng F, Guo Q, Yu Y, Ohishi Y, Qin W, Qin G, Over 50 W all-fiber mid-infrared supercontinuum laser, Opt. Express 31, 31082–31091 (2023). https://doi.org/10.1364/OE.498183.

8 Pecile VF, Leskowschek M, Modsching N, Wittwer VJ, Südmeyer T, Heckl OH, Record-high power, low phase noise synchronously-pumped optical parametric oscillator tunable from 2.7 to 4.7 μm, Appl. Phys. Lett. 125 (23), 231108 (2024). https://doi.org/10.1063/5.0233247.

9 Scalari G, Faist J, 30 years of the quantum cascade laser, Commun. Phys. 7, 394 (2024). https://doi.org/10.1038/s42005-024-01888-z.

10 Lemieux-Tanguay M, Boilard T, Paradis P, Vallée R, Bernier M, 2 W monolithic fiber laser at 3.8 μm, APL Photon. 9(7), 071301 (2024). https://doi.org/10.1063/5.0212455.

11 Qin Z, Zhou Y, Xie G, Yuan P, Ma J, Qian L, Red-diode-clad-pumped CW and mode-locked Er:ZBLAN fiber laser at 3.5 μm, Opt. Express 30(7), 11174–11180 (2022). https://doi.org/10.1364/OE.454521.

12 Henderson-Sapir O, Munch J, Ottaway DJ, Mid-infrared fiber lasers at and beyond 3.5 μm using dual-wavelength pumping, Opt. Lett. 39(3), 493–496 (2014). https://doi.org/10.1364/OL.39.000493.

13 Henderson-Sapir O, Ottaway DJ, A decade of mid-infrared, 3.5 μm dual-wavelength pumped fiber lasers, review and perspective, APL Photonics 9(10), 100901 (2024). https://doi.org/10.1063/5.0232437.

14 Lemieux-Tanguay M, Fortin V, Boilard T, Paradis P, Maes F, Talbot L, Vallée R, Bernier M, 15 W monolithic fiber laser at 3.55 μm, Opt. Lett. 47(2), 289–292 (2022). https://doi.org/10.1364/OL.446769.

15 Henderson-Sapir O, Jackson SD, Ottaway DJ, Versatile and widely tunable mid-infrared erbium doped ZBLAN fiber laser, Opt. Lett. 41(7), 1676–1679 (2016). https://doi.org/10.1364/OL.41.001676.

16 Zhang L, Fu S, Sheng Q, Luo X, Zhang J, Shi W, Yao J, Wavelength extension of Er-doped fluoride fiber laser to above 3,800 nm, J. Lightwave Technol. 42(23), 8435–8441 (2024). https://doi.org/10.1364/JLT.42.008435.

17 Zhang L, Fu S, Sheng Q, Luo X, Zhang J, Shi W, Yao J, Widely tunable single-frequency Er-doped ZBLAN fiber laser with emission from 3.37 to 3.72 μm, Opt. Lett. 48(23), 6200–6203 (2023). https://doi.org/10.1364/OL.505803.

18 Zhang L, Fu S, Sheng Q, Luo X, Zhang J, Shi C, Shi W, Yao J, 4.5 W Er-doped ZBLAN fiber laser at 3.78 μm, Opt. Lett. 50(7), 2125–2128 (2025). https://doi.org/10.1364/OL.554676.

19 Maes F, Fortin V, Bernier M, Vallée R, 5.6 W monolithic fiber laser at 3.55 μm, Opt. Lett. 42(11), 2054–2057 (2017). https://doi.org/10.1364/OL.42.002054.

20 Maes F, Stihler C, Pleau L-P, Fortin V, Limpert J, Bernier M, Vallée R, 3.42 μm lasing in heavily-erbium-doped fluoride fibers, Opt. Express 27(3), 2170–2183 (2019). https://doi.org/10.1364/oe.27.002170.

21 Froemel P, Baumann R, Lasagni AF, Eilzer S, Polarization maintaining fiber beam delivery for direct laser interference patterning, J. Laser Appl. 36(4), 042060 (2024). https://doi.org/10.2351/7.0001580.

22 Sumihara KA, Okubo S, Okano M, Inaba H, Watanabe S, Polarization-sensitive dual-comb spectroscopy, J. Opt. Soc. Am. B 34(1), 154–159 (2017). https://doi.org/10.1364/OE.27.035141.

23 Normani S, Idlahcen S, Loiko P, Hatim S, Hanzard PH, De Paula AR, Guillemot L, Godin T, Berthelot T, Cozic S, Poulain S, Hideur A, 2.8-μm polarization-maintaining Er fiber laser mode-locked by a GaSb-based SESAM, Opt. Express 32(9), 15106–15114 (2024). https://doi.org/10.1364/OE.517526.

24 Luo H, Wang Y, Li J, Liu Y, High-stability, linearly polarized mode-locking generation from a polarization-maintaining fiber oscillator around 2.8 μm, Opt. Lett. 46 (18), 4550–4553 (2021). https://doi.org/10.1364/OL.434999.

25 Luo HY, Wang YZ, Linearly polarized polarization-maintaining Er^{3+}-doped fluoride fiber laser in the mid-infrared, J. Electron. Sci. Technol. 20(1), 100147 (2022). https://doi.org/10.1016/j.jnlest.2021.100147.

26 Gauthier JC, Robichaud LR, Fortin V, Vallé R, Bernie M, Mid-infrared supercontinuum generation in fluoride fiber amplifiers: current status and future perspectives, Appl. Phys. B 124, 122 (2018). https://doi.org/10.1007/s00340-018-6980-3.

27 Ruffin PB, Sung CC, Temperature effect on the performance of polarization-maintaining fibers, Opt. Eng. 32(3), 574–579 (1993). https://doi.org/10.1117/12.61036.